Electronic Supplementary Material (ESI) for Dalton Transactions.

Supplementary Information for:

Self-assembly of a mixed-valence Fe^{II}-Fe^{III} tetranuclear star

Darunee Sertphon,[a,b] Phimphaka Harding,[a] Keith S. Murray,[c] Boujemaa Moubaraki,[c]
Nicholas F. Chilton,[d] Stephen Hill,[e,f] Jonathan Marbey,[e,f] Harry Adams,[g]
Casey G. Davies,[h] Guy N. L. Jameson[h,i] and David J. Harding*[a]

[a] Functional Materials and Nanotechnology Center of Excellence, Walailak University, Thasala, Nakhon Si Thammarat, 80160, Thailand
[b] Now at: Department of Chemistry, Faculty of Science, Rangsit University, Phaholyothin Rd., Muang, Pathum Thani, 12000, Thailand
[c] School of Chemistry, Monash University, Clayton, Victoria, 3800, Australia
[d] School of Chemistry and Photon Science Institute, The University of Manchester, Oxford Road, Manchester M13 9PL, United Kingdom
[e] Florida State University, Department of Physics, Tallahassee, FL 32306 USA
[f] National High Magnetic Field Laboratory, 1800 E. Paul Dirac Drive, Tallahassee, FL 32310, USA
[g] Department of Chemistry, University of Sheffield, Sheffield, S3 7HF, United Kingdom
[h] Department of Chemistry & MacDiarmid Institute for Advanced Materials and Nanotechnology, University of Otago, PO Box 56, Dunedin, 9054, New Zealand
[i] School of Chemistry, Bio21 Molecular Science and Biotechnology Institute, 30 Flemington Road, The University of Melbourne, Parkville Victoria 3010, Australia

E-mail: hdavid@mail.wu.ac.th
Website: https://www.funtechwu.com

Contents

Experimental Details

General Remarks 2-H_2imap was prepared as previously reported. All other chemicals were purchased from Sigma-Aldrich Chemical Company or TCI Chemicals and used as received. All compounds were prepared in air using reagent grade solvents. Elemental analyses were carried out on a Eurovector EA3000 analyser by staff of the School of Chemistry, University of Bristol, UK. ESI-MS were carried out on a Bruker Daltonics 7.0T Apex 4 FTICR Mass Spectrometer by staff at the National University of Singapore.

Synthesis of $[Fe_4(2\text{-Himap})_6][NO_3]_3$ 1

Crystals of **1** were synthesized by layered diffusion. To a solution of 2-H_2imap (0.329 g, 1.5 mmol) in MeOH (2 mL) was added Et_3N (0.21 mL, 1.0 mmol) with blank MeOH (5 mL) layered above this. A solution of $Fe(NO_3)_3{\cdot}9H_2O$ (0.0404 g, 1.0 mmol) in MeOH (5 mL) was layered on top and the test tube sealed. The solution was left for 1 week at 30 °C yielding black crystals which were washed with cold MeOH (2×2 mL), diethyl ether (2×2 mL) and air dried, yield 0.350 g (67%). ν_{max} (KBr)/cm^{-1} 3125, 3050, 2916, 1597, 1462, 1361, 1245, 1115. λ_{max}/nm (MeOH, ε / M^{-1}cm^{-1}) 306 (9000), 435 (4500). ESI-MS (MeOH) m/z = 1355.3 (**1**+H_2O-3NO_3^--2H^+), 1337.8 (**1**-3NO_3^--2H^+). Anal. Calc. for $C_{60}H_{52}N_{21}O_{17}Fe_4$ (**1**·2H_2O): C, 46.12; H, 3.35; N, 18.82. Found: C, 46.19; H, 3.36; N, 18.34%.

Crystals of $[Fe(2\text{-Himap})_2]NO_3{\cdot}0.7MeOH$ **2** were prepared in an identical manner to **1** except using 2 equivalents of 2-H_2imap and heating the reaction mixture at ~40 °C overnight. ESI-MS (MeOH) m/z = 428 (**2**). Anal. Calc. for $C_{21}H_{20}N_7O_6Fe$: C, 48.64; H, 3.58; N, 19.37. Found: C, 48.35; H, 3.73; N, 18.59%.

Crystal data and Structures

Crystals of **1** or **2** were mounted on a glass fibre using perfluoropolyether oil and cooled rapidly to 123 K in a stream of cold nitrogen for **2** only, while **1** was collected at 296 K. The diffraction data of **1** and **2** were collected on a Bruker APEXII area detector with graphite monochromated MoKα (λ = 0.71073 Å).[1] After data collection, in each case an empirical absorption correction (SADABS) was applied.[2] The structures were then solved by direct methods and refined on all F^2 data using the SHELX suite of programs[3,4] or OLEX2.[5] In all cases non-hydrogen atoms were refined with anisotropic thermal parameters; hydrogen atoms were included in calculated positions and refined with isotropic thermal parameters which were *ca*. 1.2 × (aromatic CH) or 1.5 × (Me, OH) the equivalent isotropic thermal parameters of their parent carbon atoms. All pictures were generated using OLEX2. The CCDC numbers for the X-ray crystallographic data presented in this paper are 1830689 and 1830690 for **1** and **2** respectively and can be obtained free of charge from the Cambridge Crystallographic Data Centre via www.ccdc.cam.ac.uk/data_request/cif.

Table S1 Crystallographic data and refinement parameters for **1** and **2**.

Empirical Formula	$C_{60}H_{48}Fe_4N_{21}O_{15}$	$C_{20.7}H_{18.8}FeN_7O_{5.7}$
Formula Weight	1526.61	512.68
Temperature /K	296	123
Crystal System	Cubic	Triclinic
Space Group	*Pa*3	*P*1
a, b, c /Å	23.080(2), 23.080(2), 23.080(2)	9.0937(7), 11.1693(9), 11.2944(10)
α, β, γ /°	90, 90 90	96.510(4), 104.934(4), 97.485(3)
Volume /Å^3	12295(4)	1085.98(16)
Z	8	2
ρ_{calc} /gcm^{-3}	1.649	1.548
μ /mm^{-1}	1.014	0.746
F(000)	6232	520
Crystal Dimensions: max, mid, min (mm)	0.31, 0.21, 0.19	0.30, 0.15, 0.004
Index ranges	$-30 \leq h \leq 4$, $-20 \leq k \leq 23$, $-7 \leq l \leq 27$	$-10 \leq h \leq 11$, $-13 \leq k \leq 13$, $-13 \leq l \leq 12$
Reflections Collected	21172	13639
Unique Data	4739 [R_{int} = 0.1443]	3909 [R_{int} = 0.0291]
Data/Restraints/Parameters	4739/26/327	3909/1/328
Goodness of fit on F^2	1.005	1.029

Final R factors [I>2σ (I)]	$R_1 = 0.0581$, $wR_2 = 0.1320$	$R_1 = 0.0375$, $wR_2 = 0.0851$
Largest residual peak/hole /eÅ^{-3}	0.548 / -0.579	0.351 /-0.313
CCDC no.	1830689	1830690

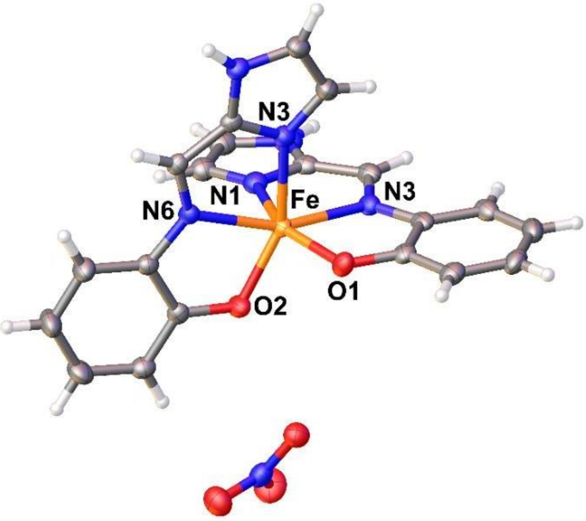

Figure S1. View of [Fe(2-Himap)$_2$]NO$_3$·0.5MeOH **2** showing the numbering of the non-C and H atoms.

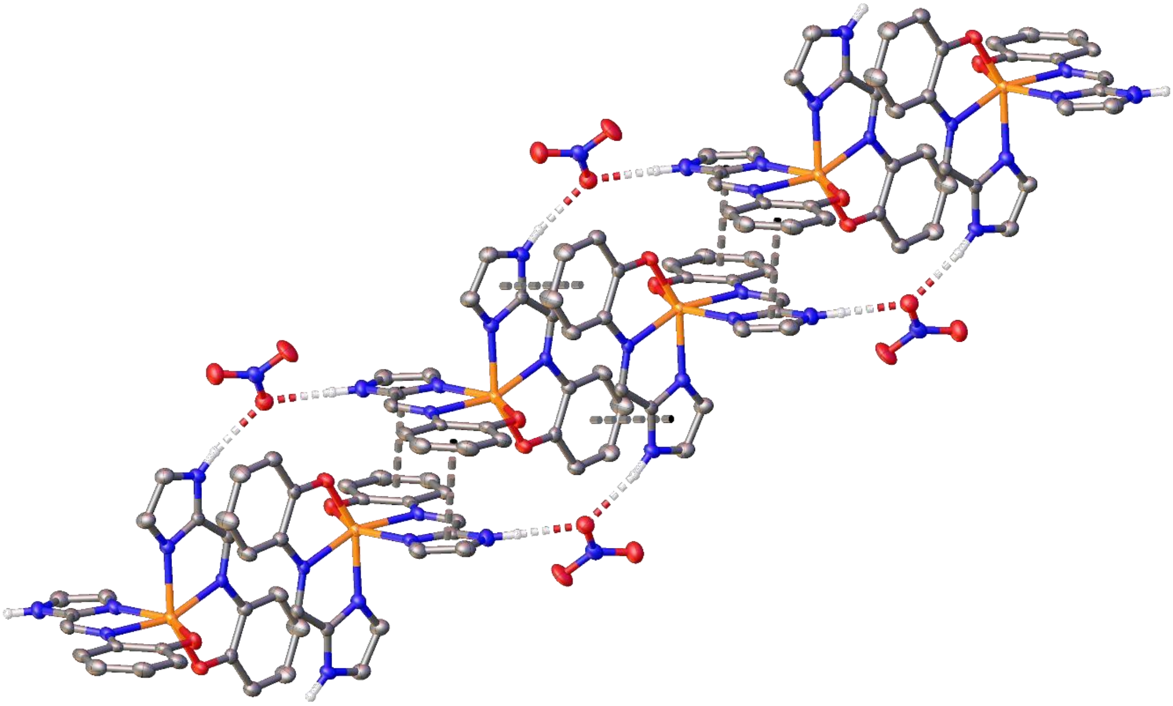

Figure S2. View of the π-π and C-H···O interactions that form the 1D chain in [Fe(2-Himap)$_2$]NO$_3$·0.5MeOH **2**.

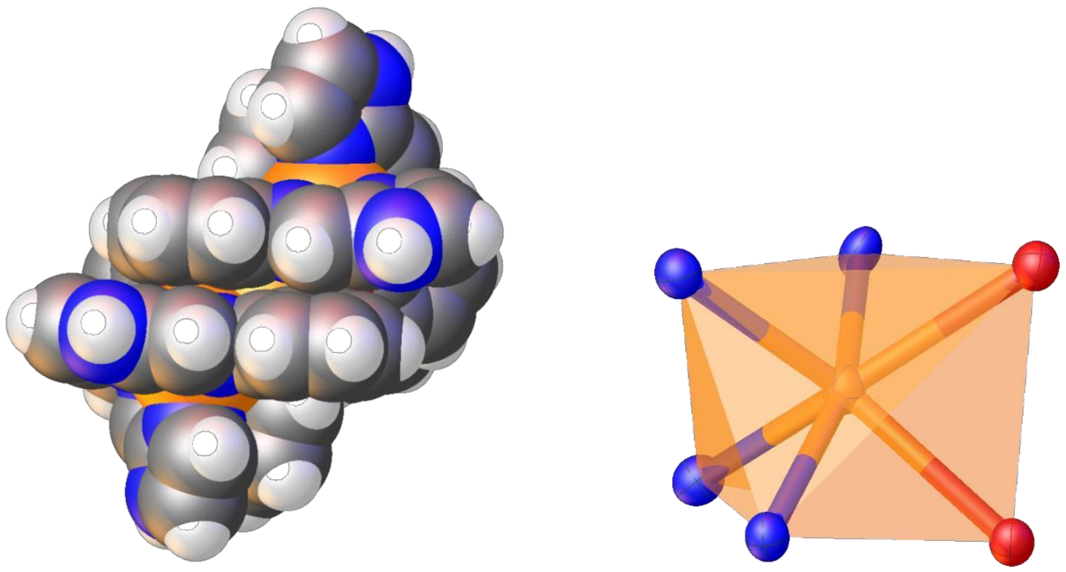

a) b)

Figure S3. a) View of one of the intramolecular π-π interactions in **1** where the plane-to-plane distance is 3.343(2) Å and b) the distorted coordination sphere at Fe2.

MS and PXRD data

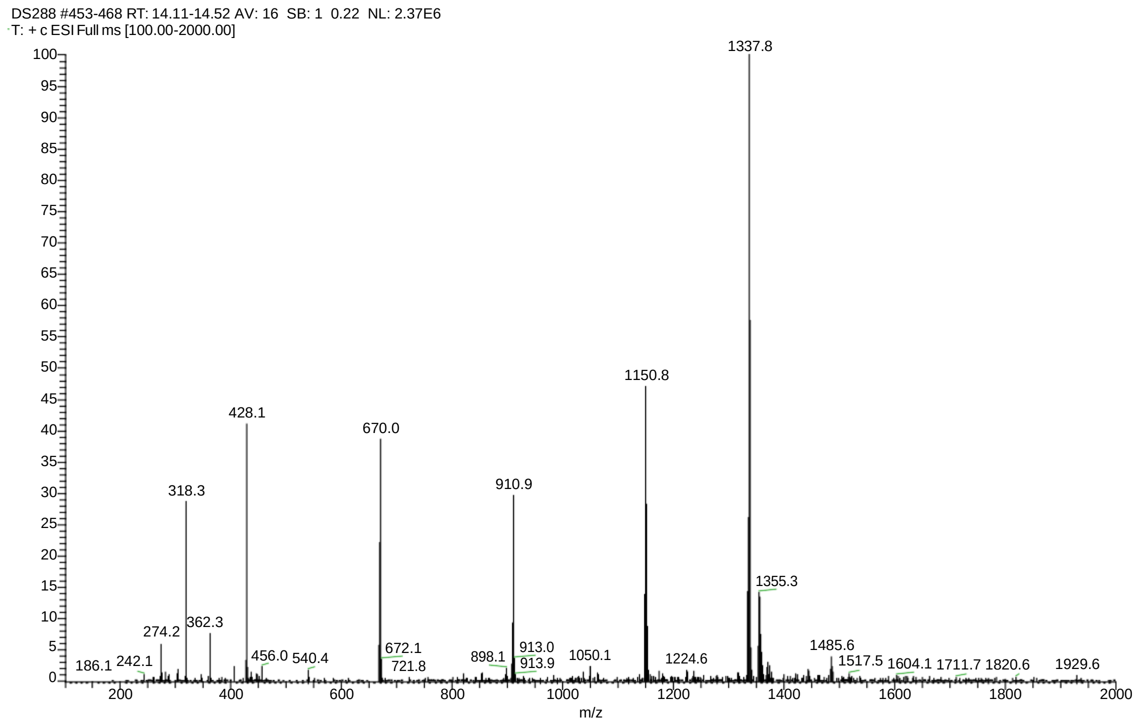

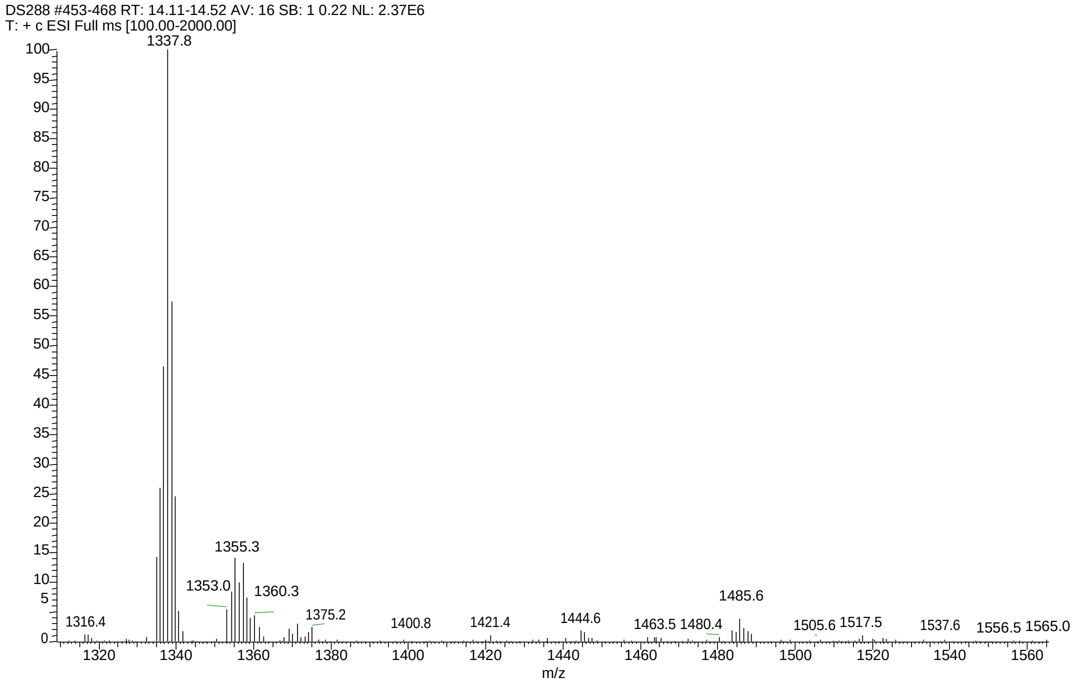

Figure S4. ESI-MS of $[Fe_4(2\text{-Himap})_6][NO_3]_3$ **1**.

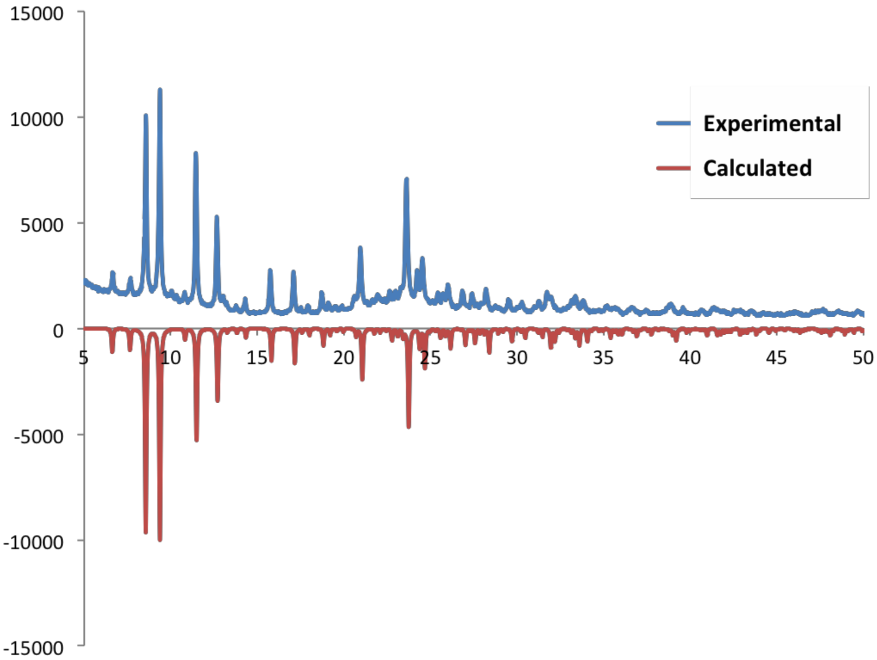

Figure S5. The observed and calculated X-ray powder patterns of $[Fe_4(2\text{-Himap})_6][NO_3]_3$ **1**.

Mössbauer spectroscopic studies

Mössbauer spectra were measured on solid samples (approximately 25 mg) held in a custom Teflon sample holder. Two different preparations were measured, and almost identical data collected. Mössbauer spectra were recorded on a spectrometer from SEE Co. (Science Engineering & Education Co., MN) equipped with a closed cycle refrigerator system from Janis Research Co. and SHI (Sumitomo Heavy Industries Ltd.). Data were collected in constant acceleration mode in transmission geometry. The zero velocity of the Mössbauer spectra refers to the centroid of the room temperature spectrum of a 25 µm metallic iron foil. Analysis of the spectra was conducted using the WMOSS program (SEE Co, formerly WEB Research Co. Edina, MN). Unless noted elsewhere, a weak magnetic field (47 mT) was applied parallel to the γ-beam.

The spectra are plotted in Figure S6, the fitted parameters are presented in Table S2 and plotted for ease of comparison in Figure S7.

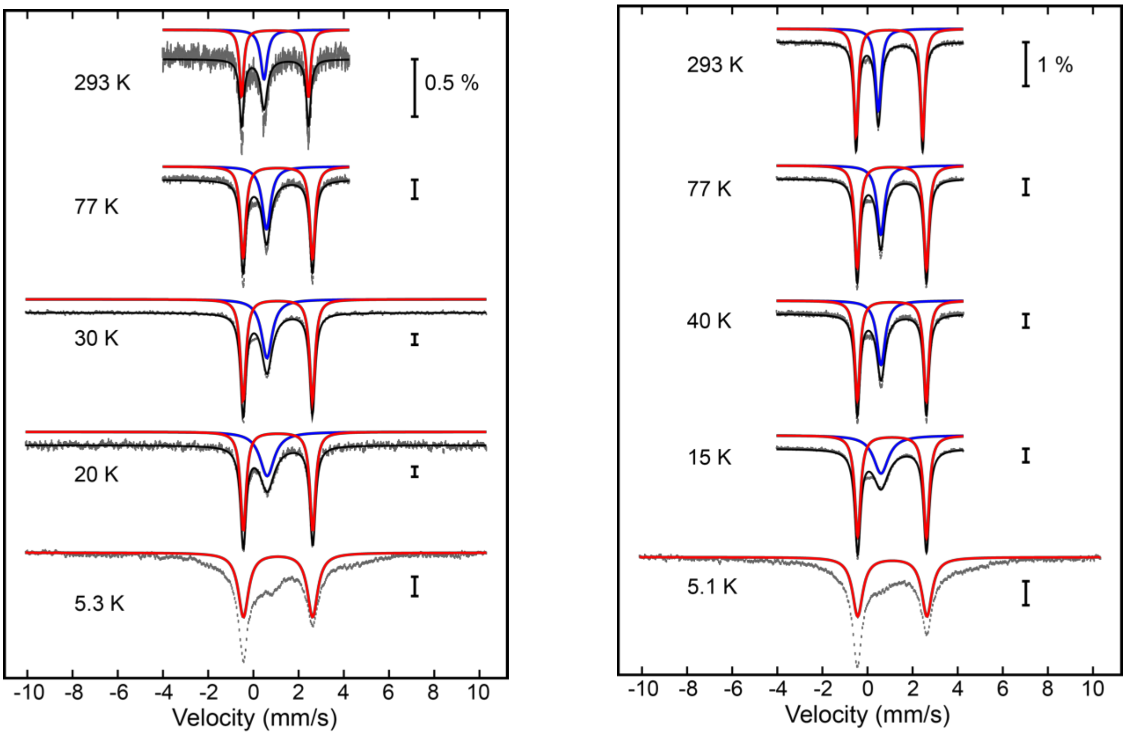

Figure S6. ^{57}Fe Mössbauer spectra of two different samples of **1** at various temperatures measure with a magnetic field of 47 mT applied parallel to the γ-beam. HS Fe^{II} (red) and HS Fe^{III} (blue).

Table S2. ^{57}Fe Mössbauer parameters obtained for [Fe$_4$(2-Himap)$_6$][NO$_3$]$_3$ **1** measured in the presence of an applied field of 47 mT parallel to the γ-beam.[a]

T (K)	δ (mm/s)	ΔE_Q (mm/s)	$\Gamma_{L=R}$ (mm/s)	I (%)
293	0.97	2.95	0.24	67
	0.48	0	0.31	33
77	1.08	3.07	0.28	67
	0.59	0	0.41	33
40	1.08	3.06	0.28	66
	0.60	0	0.45	34
15	1.09	3.05	0.31	68
	0.60	0	0.80	32
5.1	1.10	3.07	0.55	35
	broad			
293	0.96	2.96	0.23	64
	0.47	0	0.35	36
77	1.08	3.07	0.29	65
	0.58	0	0.46	35
30	1.08	3.06	0.29	64
	0.60	0	0.57	36
20	1.09	3.07	0.30	64
	0.61	0	0.77	36
5.1	1.09	3.06	0.55	38
	broad			

[a] Two independent samples have been measured.

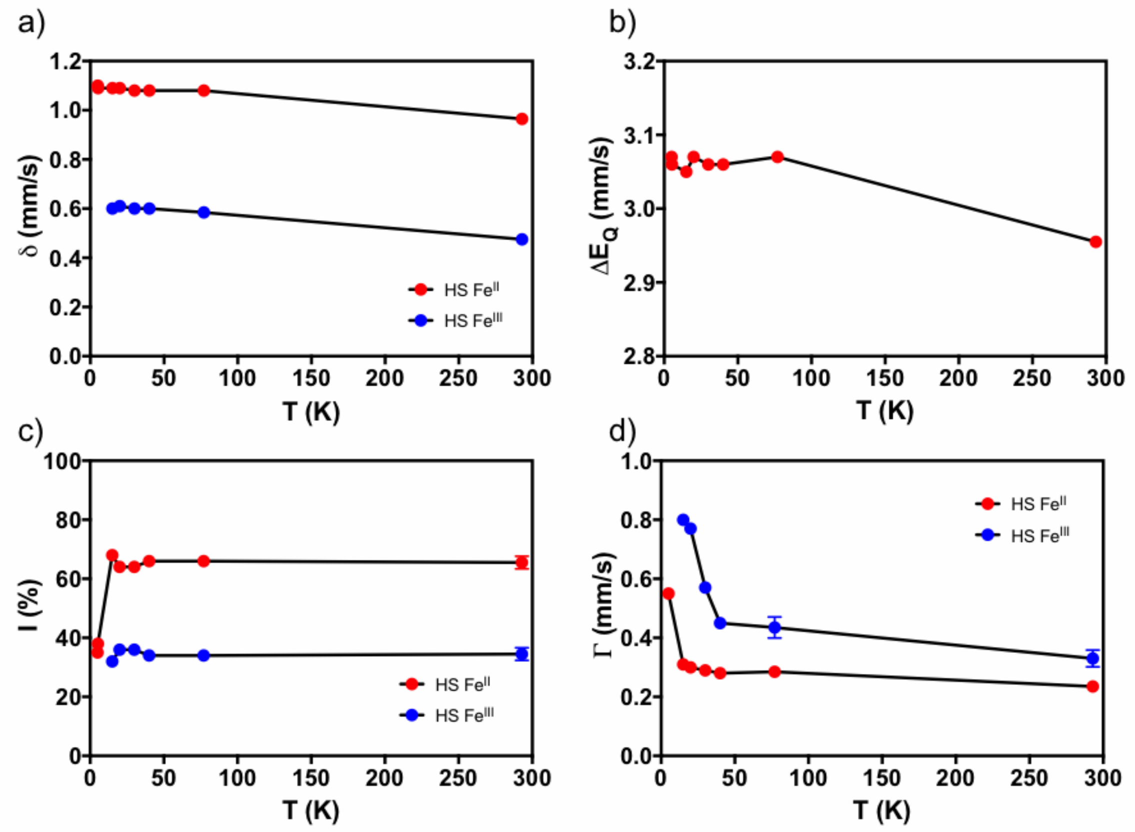

Figure S7. The temperature dependence of the fitted parameters are presented. a) The isomer shift (δ) shows a second order Doppler shift. b) The quadrupole splitting (ΔE_Q) of the Fe^{ii} sub-spectra shows a decrease with increasing temperature commonly observed. c) The intensity (I) is constant at 2:1 (Fe^{II}:Fe^{III}) across both samples and all temperatures except very low temperatures. d) The half-height widths (Γ) show a large increase at low temperatures consistent with a switch to intermediate relaxation.

Magnetic studies

Variable-temperature magnetic susceptibility measurements were performed on a Quantum Design MPMS 7T SQUID magnetometer over the temperature range 2 to 300 K and in applied DC fields of 0.1 and 1.0 T. The SQUID magnetometer was calibrated by use of a standard palladium sample (Quantum Design) of accurately known magnetization or by use of magnetochemical calibrants such as $CuSO_4 \cdot 5H_2O$. Microcrystalline samples were dispersed in Vaseline in order to avoid torquing of the crystallites. The sample mulls were contained in a calibrated capsule held at the centre of a drinking straw that was fixed at the end of the sample rod. AC measurements of in-phase and out-of-phase susceptibilities were made between 1.8 and 10 K in frequencies of 50-1500 Hz under zero DC field and in an applied DC field of 3000 Oe.

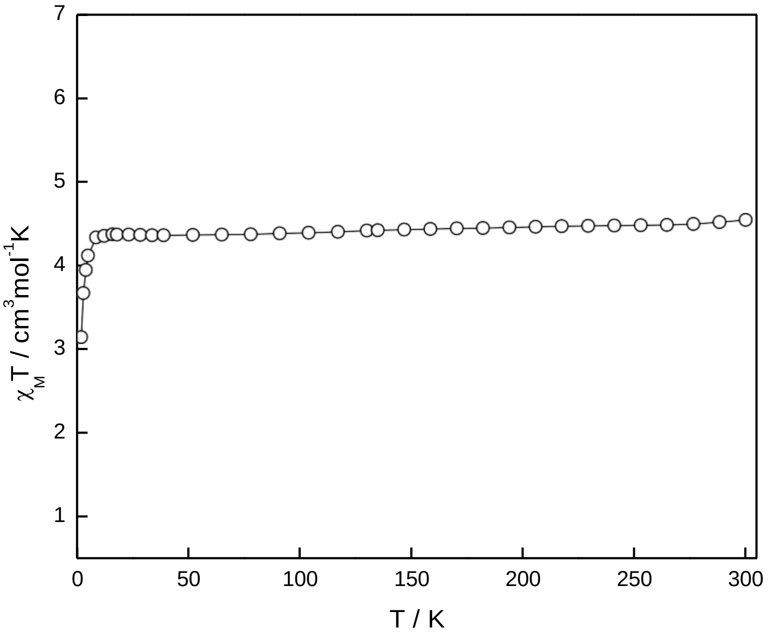

Figure S8. χ_MT vs. T plot of $[Fe(2\text{-}Himap)_2]NO_3 \cdot 0.7MeOH$ **2**.

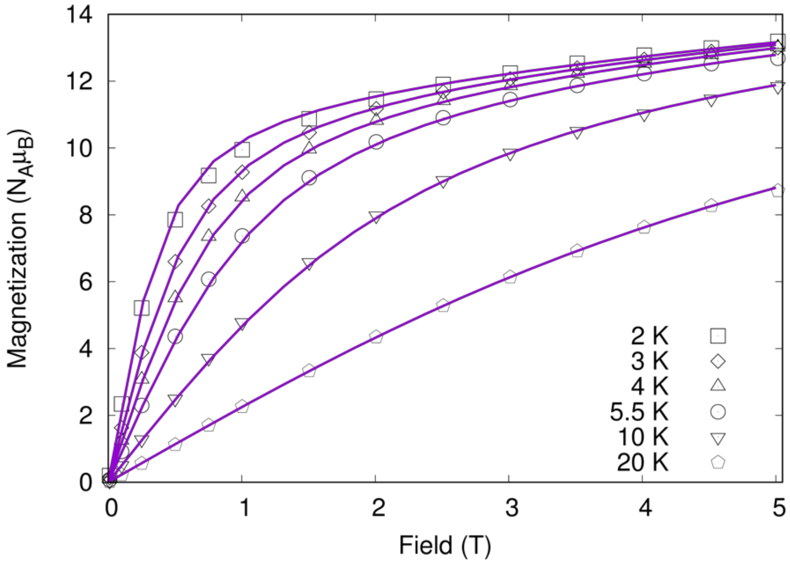

Figure S9. *M* vs. B plot of **1**. Purple lines are fits using *D* < 0 model; parameters are given in main text.

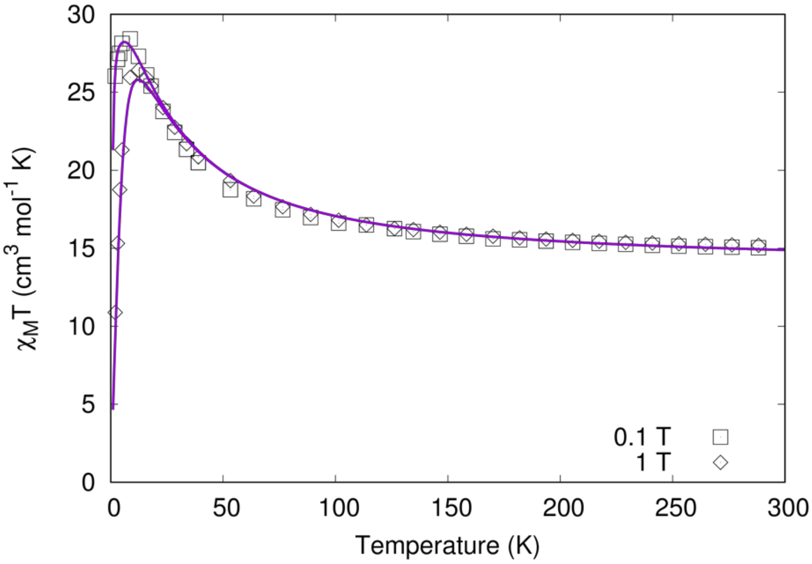

Figure S10. χ_MT vs. T plot of **1**. Purple lines are fits using *D* > 0 model; parameters are given in main text.

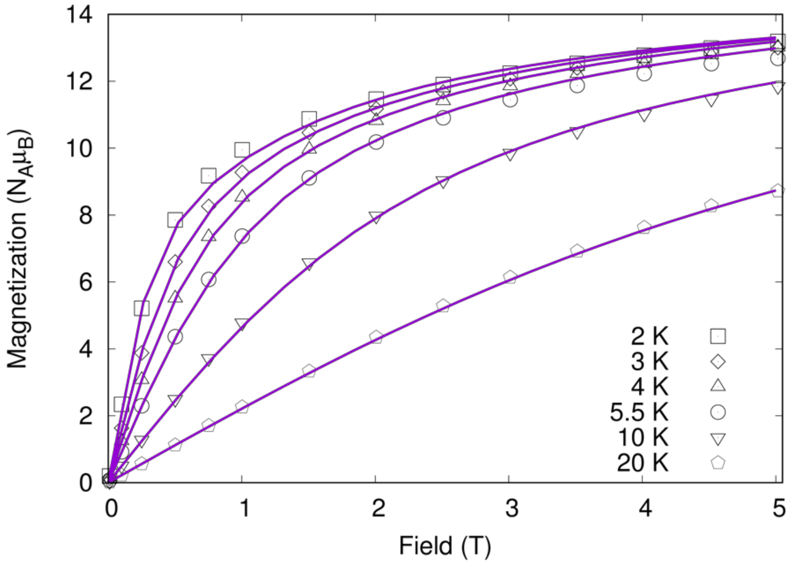

Figure S11. *M* vs. B plot of **1**. Purple lines are fits using *D* > 0 model; parameters are given in main text.

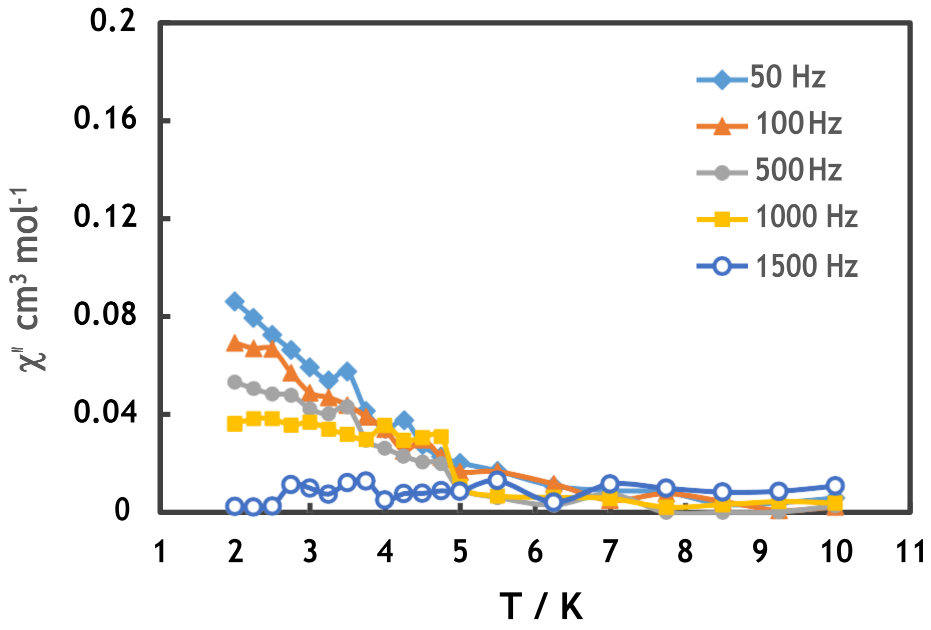

Figure S12. Plot of χ'' versus temperature for **1** at frequencies of 50-1500 Hz under an applied *dc* field of 3000 Oe.

CASSCF-SO calculations

CASSCF-SO calculations were performed with MOLCAS 8.0,[6ref] using the crystal structure of **1** with no optimization. Calculations were performed for the unique peripheral Fe^{II} site, where the central Fe^{III} was replaced with diamagnetic Ga^{III} and the other Fe^{II} sites with diamagnetic Zn^{II}. The basis set for Fe was ANO-RCC-VTZP, those for the first coordination sphere were ANO-RCC-VDZP, those for the rest of the non-hydrogen atoms were ANO-RCC-VDZ, and ANO-RCC-MB for the hydrogen atoms.[7–9ref] The two-electron integrals were Cholesky decomposed with the default thresholds to save computational resources. The active space was 6 electrons in the 3d orbitals, considering 5 roots for the $S = 4$ states, 45 roots for the $S = 1$ states, and 50 roots for the $S = 0$ states, all in state-averaged CASSCF calculations. All states were then mixed by spin-orbit coupling. The ZFS and g-values were calculated with single_aniso.[10]

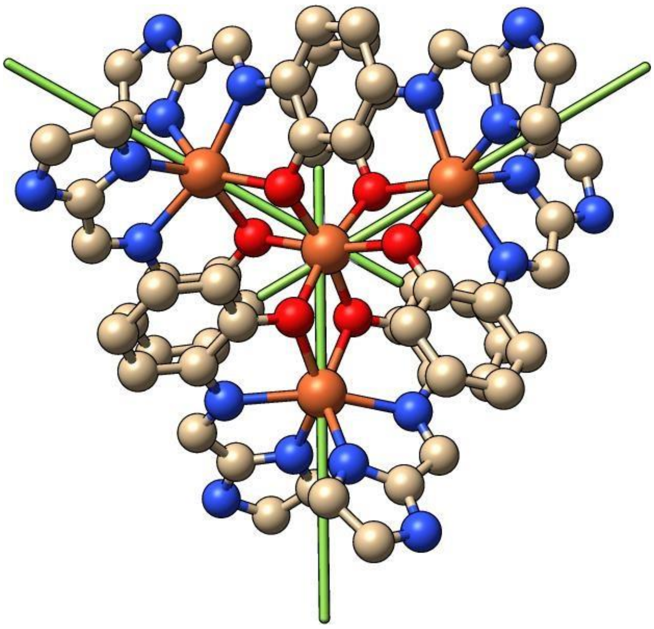

Figure S13. View of the main anisotropic axes at each of the peripheral Fe^{II} centres.

EPR spectroscopic studies

Variable temperature, multi-high-field/frequency EPR measurements were performed on a constrained powder of **1** using a transmission-type set up. Microwaves in the 52-435 GHz range were generated via a phase-locked 13±1 GHz source (Virginia Diodes, Inc.), which was upconverted via a cascade of multipliers in order to reach the desired frequency.[11] A Backward-Wave Oscillator (BWO) source was employed for the higher frequencies in the range 600–700 GHz. A liquid helium cooled InSb bolometer was used as a microwave detector, and the instrument is equipped with a superconducting magnet capable of reaching a field of 14 T. All spectra were recorded in derivative mode, dI/dB (where I is the absorption intensity), using field modulation and lock-in detection. Temperature regulation was achieved by means of a variable flow helium cryostat.

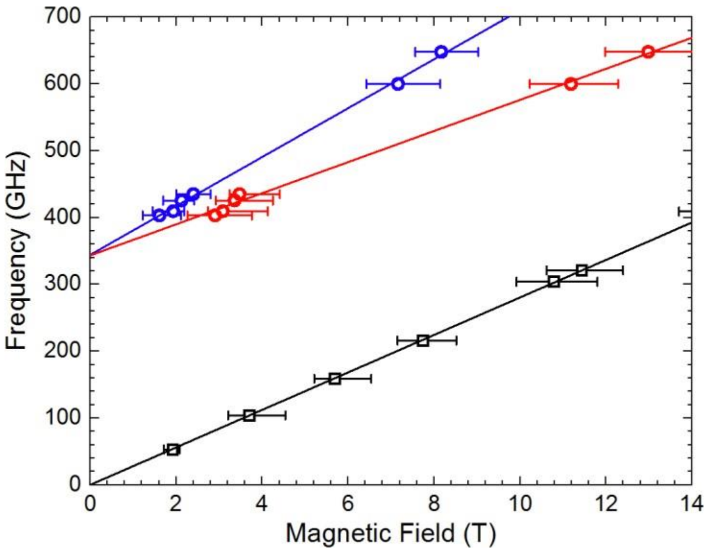

Figure S14. Frequency dependence of the resonance positions (in field) deduced from the spectra in Figure 3.

References

1 *Bruker APEXII*, Bruker AXS Inc., Madison, WI, USA, 2005.

2 *SADABS and SAINT*, Bruker AXS Inc., Madison, WI, USA, 2003.

3 G. M. Sheldrick, *Acta Crystallogr. Sect. C Struct. Chem.*, 2015, **71**, 3–8.

4 G. M. Sheldrick, *Acta Crystallogr. Sect. A Found. Crystallogr.*, 2015, **71**, 3–8.

5 O. V. Dolomanov, L. J. Bourhis, R. J. Gildea, J. A. K. Howard and H. Puschmann, *J. Appl. Cryst.*, 2009, **42**, 339–42.

6 F. Aquilante, J. Autschbach, R. K. Carlson, L. F. Chibotaru, M. G. Delcey, L. De Vico, I. Fdez. Galván, N. Ferré, L. M. Frutos, L. Gagliardi, M. Garavelli, A. Giussani, C. E. Hoyer, G. Li Manni, H. Lischka, D. Ma, P. Å. Malmqvist, T. Müller, A. Nenov, M. Olivucci, T. B. Pedersen, D. Peng, F. Plasser, B. Pritchard, M. Reiher, I. Rivalta, I. Schapiro, J. Segarra-Martí, M. Stenrup, D. G. Truhlar, L. Ungur, A. Valentini, S. Vancoillie, V. Veryazov, V. P. Vysotskiy, O. Weingart, F. Zapata and R. Lindh, *J. Comput. Chem.*, 2016, **37**, 506–541.

7 B. O. Roos, V. Veryazov and P.-O. Widmark, *Theor. Chem. Acc.*, 2004, **111**, 345–351.

8 B. O. Roos, R. Lindh, P.-Å. Malmqvist, V. Veryazov and P.-O. Widmark, *J. Phys. Chem. A*, 2004, **108**, 2851–2858.

9 B. O. Roos, R. Lindh, P.-Å. Malmqvist, V. Veryazov and P.-O. Widmark, *J. Phys. Chem. A*, 2005, **109**, 6575–6579.

10 L. F. Chibotaru and L. Ungur, *J. Chem. Phys.*, 2012, **137**, 64112.

11 A. Hassan, L. Pardi, J. Krzystek, A. Sienkiewicz, P. Goy, M. Rohrer and L.-C. Brunel, *J. Magn. Reson.*, 2000, **142**, 300–312.